Competitive Tuning Among Ca^{2+}/Calmodulin-Dependent Proteins: Analysis of *In Silico* Model Robustness and Parameter Variability

Matthew C. Pharris, Neal M. Patel, and Tamara L. Kinzer-Ursem

Weldon School of Biomedical Engineering, Purdue University, 260 South Martin Jischke Drive, West Lafayette, IN 47907, USA

Abstract

Introduction—Calcium/calmodulin-dependent (Ca^{2+}/CaM-dependent) regulation of protein signaling has long been recognized for its importance in a number of physiological contexts. Found in almost all eukaryotic cells, Ca^{2+}/CaM-dependent signaling participates in muscle development, immune responses, cardiac myocyte function and regulation of neuronal connectivity. In excitatory neurons, dynamic changes in the strength of synaptic connections, known as synaptic plasticity, occur when calcium ions (Ca^{2+}) flux through NMDA receptors and bind the Ca^{2+}-sensor calmodulin (CaM). Ca^{2+}/CaM, in turn, regulates downstream protein signaling in actin polymerization, receptor trafficking, and transcription factor activation. The activation of downstream Ca^{2+}/CaM-dependent binding proteins (CBPs) is a function of the frequency of Ca^{2+} flux, such that each CBP is preferentially "tuned" to different Ca^{2+} input signals. We have recently reported that competition among CBPs for CaM binding is alone sufficient to recreate *in silico* the observed *in vivo* frequency-dependence of several CBPs. However, CBP activation may strongly depend on the identity and concentration of proteins that constitute the competitive pool; with important implications in the regulation of CBPs in both normal and disease states.
Methods—Here, we extend our previous deterministic model of competition among CBPs to include phosphodiesterases, AMPAR receptors that are important in synaptic plasticity, and enzymatic function of CBPs: cAMP regulation, kinase activity, and phosphatase activity. After rigorous parameterization and validation by global sensitivity analysis using Latin Hypercube Sampling (LHS) and Partial Rank Correlation Coefficients (PRCC), we explore how perturbing the competitive pool of CBPs influences downstream signaling events. In particular, we hypothesize that although perturbations may decrease activation of one CBP, increased activation of a separate, but enzymatically-related CBP could compensate for this loss, providing a homeostatic effect.
Results and Conclusions—First we compare dynamic model output of two models: a two-state model of Ca^{2+}/CaM binding and a four-state model of Ca^{2+}/CaM binding. We find that a four-state model of Ca^{2+}/CaM binding best captures the dynamic nature of the rapid response of CaM and CBPs to Ca^{2+} flux in the system. Using global sensitivity analysis, we find that model output is robust to parameter variability. Indeed, although variations in the expression of the CaM buffer neurogranin (Ng) may cause a decrease in Ca^{2+}/CaM-dependent kinase II (CaMKII) activation, overall AMPA receptor phosphorylation is preserved; ostensibly by a concomitant increase in adenylyl cyclase 8 (AC8)-mediated activation of protein kinase A (PKA). Indeed phosphorylation of AMPAR receptors by CaMKII and PKA is robust across a wide range of Ng concentrations, though increases in AMPAR phosphorylation is seen at low Ng levels approaching zero. Our results may explain recent counter-intuitive results in neurogranin knockout mice and provide further evidence that competitive tuning is an important

Address correspondence to Tamara L. Kinzer-Ursem, Weldon School of Biomedical Engineering, Purdue University, 260 South Martin Jischke Drive, West Lafayette, IN 47907, USA. Electronic mail: tursem@purdue.edu

Tamara L. Kinzer-Ursem is an Assistant Professor in the Weldon School of Biomedical Engineering. She received her B.S. in Bioengineering from the University of Toledo, M.S. and Ph.D. degrees in Chemical Engineering from the University of Michigan, and her post-doctoral training in Molecular Neuroscience at the California Institute of Technology. Prior to joining Purdue she was the Head of R&D in Biochemistry at Maven Biotechnologies and Visiting Associate in Chemical Engineering at the California Institute of Technology. Research in the Kinzer-Ursem lab focuses on developing tools to advance quantitative descriptions of cellular processes and disease within three areas of expertise: (1) Computational modeling of signal transduction mechanisms to understand cellular processes. Using computational techniques, we have recently described "competitive tuning" as a mechanism that might be used to regulate information transfer through protein networks, with implications in cell behavior and drug target analysis; (2) Development of novel protein tagging technologies that are used to label proteins *in vivo* to enable quantitative description of protein function and elucidate disease mechanisms; and (3) Using particle diffusivity measurements to quantify biomolecular processes. Particle diffusometry is being used as a sensitive biosensor to detect the presence of pathogens in environmental and patient samples.

This article is part of the 2018 CMBE Young Innovators special issue.

mechanism in synaptic plasticity. These results may be readily translated to other Ca^{2+}/CaM-dependent signaling systems in other cell types and can be used to suggest targeted experimental investigation to explain counter-intuitive or unexpected downstream signaling outcomes.

Keywords—Signal transduction, Dendritic spine, Calcium signaling, Adenylyl cyclase, Ca^{2+}/calmodulin-dependent kinase II (CaMKII), Neurogranin.

ABBREVIATIONS

AC1	Adenylyl cyclase 1
AC8nt, AC8ct	Adenylyl cyclase 8N/C-terminus
AMPAR	α-Amino-3-hydroxy-5-methyl-4-isoxazolepropionic acid receptor
Ca^{2+}	Calcium ion
CaM	Calmodulin
CBP	Calmodulin binding protein
CaMKII	Calcium/calmodulin-dependent protein kinase II
CaN	Calcineurin
Inh-1	Inhibitor 1
LTP	Long-term potentiation
MLCK	Myosin light chain kinase
NOS	Nitric oxide synthetase
Ng	Neurogranin
NMDAR	*N*-methyl-D-aspartic acid receptor
PDE1, PDE4	Phosphodiesterase 1/4
PKA	Protein kinase A
PP1	Protein phosphatase 1

INTRODUCTION

Worldwide, as many as 1 billion people suffer from neurological disorders.[52] In the US alone, neurological disorders affect more than 1 in 7 households.[4] At the most basic level, these neurological disorders arise from perturbations in protein signaling networks within neuronal synapses. Normal synaptic function requires dynamic, short-timescale regulation of the connective strength of the synapse. This regulation is initiated within the post-synapse by the influx of calcium ions (Ca^{2+}) through NMDA receptors.[19] Intracellular Ca^{2+} binds the Ca^{2+} sensor protein calmodulin (CaM), which subsequently activates a variety of Ca^{2+}/CaM-dependent protein signaling pathways. Ca^{2+}/CaM-dependent pathways may either potentiate synaptic connective strength *via* AMPA receptor (AMPAR) phosphorylation and trafficking to the synapse, or they may depress synaptic strength by regulating AMPAR de-phosphorylation and removal from

the synapse (recently reviewed in Huganir and Nicoll[21]). Although many of the proteins that are involved in Ca^{2+}/CaM-dependent AMPAR regulation are well known, the dynamics of the pathway(s) are far from understood. With computer-guided studies, we begin to characterize the dynamics and cross-talk inherent to the protein interactions in these pathways, possibly enabling the identification of new therapeutic targets for treating neurological disorders.

Calmodulin (CaM) regulates synaptic plasticity by selectively activating a number of downstream proteins, termed calmodulin binding proteins (CBPs), within the signaling networks responsible for either the dynamic strengthening or weakening of synaptic connections. The binding of CaM to its many downstream binding partners[9,15,27,53] depends on the kinetic rates with which different CaM species bind CBPs, such that each CBP is preferentially activated by, or "tuned" to, different input Ca^{2+} signals. Aside from binding dynamics, other mechanisms that regulate this tuning include feedback loops, spatial localization, and a recently described phenomenon called competitive tuning.[22,45,46] We have recently reported that competitive tuning is sufficient to recreate, *in silico*, the *in vivo* Ca^{2+} frequency-dependence of several CBPs.[45] One prediction from competitive tuning is that, in the absence of other mechanisms, signaling outcomes may strongly depend on the abundance and binding dynamics of individual CBPs; parameters susceptible to perturbation either by genetic regulation or by post-translational modification. It follows then that signaling outcomes may lack robustness if competitive tuning occurs in isolation of other regulatory mechanisms.

Indeed, modulating just one parameter (e.g., a protein's concentration) could cause a shift in competition that influences the signaling outcomes of other proteins in the system, perhaps leading to non-intuitive effects. We have previously shown that simulated knockout of the CaM buffer neurogranin (Ng) shifts the competition for CaM, non-intuitively decreasing Ca^{2+}/CaM-dependent kinase II (CaMKII) activation and concomitantly increasing adenylyl cyclase (AC) activation.[45] Our previous results may explain a surprising experimental observation by Krucker *et al.*[26] in which Ng knockout (Ng KO) mice retain the ability to acquire long-term potentiation (LTP), despite a considerable reduction in CaMKII activity.[26] In this present work we further explore how competitive tuning regulates LTP, hypothesizing that although reduced CaMKII activation in the Ng KO should reduce the phosphorylation of AMPA receptor GluA1 subunits at residue S831, a coincident increase in AC activation may cause an increase in GluA1 subunit phosphorylation at residue S845. This would lead to robustness in the overall level of GluA1 phosphorylation. Although

there is still some debate about the precise roles of phosphorylation at S831 and S845, it is well accepted that phosphorylation of these sites is involved in the function and location of AMPARs and in synaptic plasticity (recently reviewed in Refs. [11] and [21]). Thus, competitive tuning alone could provide the mechanism by which overall GluA1 phosphorylation levels are maintained and provide a homeostatic effect on synaptic plasticity.

Here, we compare two models of Ca2 +/CaM-dependent activation of CBPs; a 2-state Ca2 +/CaM binding model and a four-state Ca2 +/CaM-binding model. We include well documented CBPs that are highly expressed in neurons, and also include signaling events downstream of Ca2 +/CaM binding, including CaM-dependent enzymatic activity, PKA kinase activation, phosphatase regulation, and AMPAR receptor phosphorylation. After validating the model, we use a global sensitivity analysis to quantify the effect of parameter perturbations on model outcomes. We also find that at short timescales, competitive tuning provides robustness in overall GluA1 phosphorylation levels *via* upregulation in the activation of PKA-mediated phosphorylation of GluA1 in conditions that simulate the Ng KO. Our results provide further evidence that competitive tuning could be an important mechanism in the regulation and maintenance of synaptic plasticity.

RESULTS AND DISCUSSION

Model Development

Model Structure

Similar to our previous work,[45] we constructed models of CaM binding to a number of downstream CBPs and allowed the CBPs to compete for the various states of Ca^{2+}/CaM. CaM has four binding sites for Ca^{2+} ions, two in EF-hand domains in the amino (N) terminus, and two in EF-hand domains in the carboxy (C) terminus. The binding of Ca^{2+} within each terminus is highly cooperative, for example upon binding of the first Ca^{2+} ion at the N-terminus, a second Ca^{2+} ion binds rapidly to the N-terminus. But binding between the termini is independent (i.e., Ca^{2+}-binding at the N-terminus does not change the binding of Ca^{2+} at the C-terminus). Many models of Ca^{2+} signaling cascades in neurons and cardiomyocytes have employed a simplified, yet still relevant model of Ca^{2+} ions binding to CaM where all four Ca^{2+} ions are assumed to bind simultaneously (outlined in Fig. 1a). These models have been used extensively and are thought to be quite accurate, at least for scenarios in which the overall magnitude of Ca^{2+} flux is large, such as in Ca^{2+}-de-

pendent Ca^{2+} release phenomena or high frequency Ca^{2+} flux. However, more detailed descriptions of CaM that account for its intermediate, sub-saturated states (outlined in Fig. 1b) may be more appropriate for situations in which Ca^{2+} flux occurs at moderate to low frequencies, or in conditions of limiting Ca^{2+}.[31] It has been shown that several CBPs (MLCK, CaMKII, AC1 and AC8) produce CaM-dependent activity even with small increases in Ca^{2+} concentration.[33,39,48] Additionally, CaMKII has been shown to be enzymatically active with only two Ca^{2+} ions bound to CaM,[13] and AC8 has been shown to bind CaM with only two Ca^{2+} ions bound to CaM.[33] These observations and the fact that binding of Ca^{2+} to CaM is highly cooperative within each terminus, but not between termini, together have led some to develop models that include more intermediate states of Ca^{2+} binding to CaM.[42,45,46]

We compare a 2-state CaM model to a 4-state CaM model (Figs 1a and 1b). For both models we view CaM as a limiting resource. There are many more CBPs than CaM itself. Thus CBPs compete simultaneously for binding to CaM in its different states (overview in Figs. 1c, 1d and 2). Listed in Table 1, the CBPs that are included in this work are highly expressed in neurons and widely reported to interact with CaM (see Ref. [53] for a review). The reactions that describe these interactions are listed in Table S1. To study downstream events in Ca^{2+}/CaM-dependent signaling we additionally include enzymatic activation of CBPs and the relevant proteins and nucleotides that are downstream of CaM-binding. These include the generation of cAMP by AC1 and AC8, hydrolysis of cAMP by PDE1 and PDE4, activation of PKA by cAMP, phosphorylation of GluA1 by PKA and CaMKII, and de-phosphorylation of GluA1 by CaN and PP1 (summarized in Table 2; reactions listed in Table S2). The interactions among Ca^{2+} ions, proteins, and nucleotides described above and shown schematically in Fig. 2 and the corresponding differential equations are found in Supplemental Material section 'Model Equations'. In total there are 91 equations and 225 parameters for the 2-state model and 151 equations and 447 parameters for the 4-state model.

Model Parameterization

Model parameters are either obtained directly from literature or are calculated from published values using the principle of microscopic reversibility and implementing the assumption that Ca^{2+} binding does not affect the rate of protein dissociation from CaM k_{off}, but rather the association rate (k_{on}) such that the general equation $K_{\mathrm{D}} = \frac{k_{\mathrm{off}}}{k_{\mathrm{on}}}$ can be used to calculate rate constants. These assumptions have been used regularly
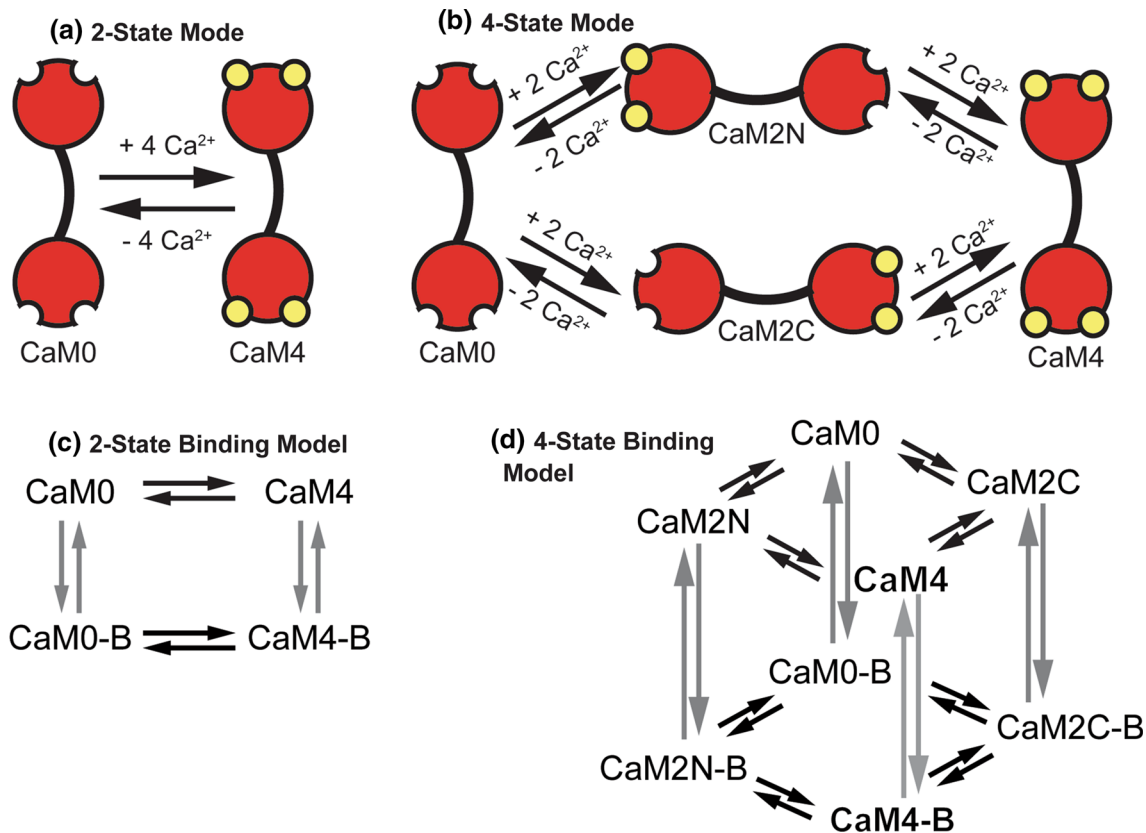
FIGURE 1. Schematic representations of binding models. (a, b) Binding models of Ca^{2+}-binding to calmodulin. Four Ca^{2+} ions (yellow circles) bind to CaM at binding sites in the amino (N) and carboxyl (C) termini. (a) 2-state model of Ca^{2+} binding to CaM. CaM with no Ca^{2+} ions bound (CaM0) is assumed to simultaneously bind four Ca^{2+} ions forming a fully saturated Ca^{2+} bound CaM (CaM4). (b) 4-state model of Ca^{2+} binding to CaM where two Ca^{2+} ions bind simultaneously to either the N- or C- termini of CaM (CaM2 N or CaM2C, respectively). In a subsequent reaction two Ca^{2+} ions bind to either termini to form fully saturated Ca^{2+}-bound CaM (CaM4). (c, d) Models of Ca^{2+} binding to CaM and CaM binding to downstream binding partners. (c) 2-state binding model where CaM0 with no Ca^{2+} ions bound binds to downstream binding partners (represented by CaM0-B). CaM4 can also bind to downstream binding partners (CaM4-B). (d) 4-state binding model where all states of CaM (CaM0, CaM2 N, CaM2C, and CaM4) may bind downstream binding partners (CaM0-B, CaM2N-B, CaM2C-B, and CaM4-B).

in the modeling literature by us and others[23,24,42,45] and have been shown to be experimentally validated.[41] For the Ca^{2+}/CaM-dependent enzymes AC, PDE1, and CaN the catalytic activity is assumed to scale with the amount of Ca^{2+} bound to CaM, similar to what has been shown with CaMKII.[48] Thus we calculate scaled values for the catalytic activity of sub-saturated Ca^{2+}-bound CaM-CBPs similar to our previous model of CaMKII auto-phosphorylation.[45] For example, the catalytic activity of Ca^{2+}/CaM$_{2C}$-CaN is slower than that of Ca^{2+}/CaM$_4$-CaN. In the absence of experimental measurement of catalytic rate constants for AC, PDE1, and CaN activity when bound to sub-saturated CaM, we calculated these scaled catalytic rate constants such that the rate of activity of the CaM$_{2C}$-bound state relative to that CaM$_4$-bound state was decreased by a similar proportion to that of the phosphorylation rate CaM$_{2C}$-CaMKII to CaM$_4$-CaMKII which has been previously measured.[48] Cat-

alytic rate constants for CaM$_{2N}$-bound state of AC, PDE1, and CaN was similarly scaled relative to the ratio of phosphorylation rate constants of CaM$_{2N}$-CaMKII to CaM$_4$-CaMKII. The values of all parameters are provided in Supplemental Table S5.

Prior to executing Ca^{2+} flux, each simulation was run for a time course of 30 s at a basal level of 5 nM Ca^{2+} to allow for steady state binding of CaM to CBPs.[32,37] The concentrations of all species at the end of this preliminary simulation were used as the input for simulations in which Ca^{2+} flux was initiated at varying frequencies.

2-State vs 4-State CaM Binding Models

In previous work we have shown that a thermodynamically complete, 9-state model of Ca^{2+} binding to CaM did not significantly change model output relative to a 4-state binding model.[45] In this work our first
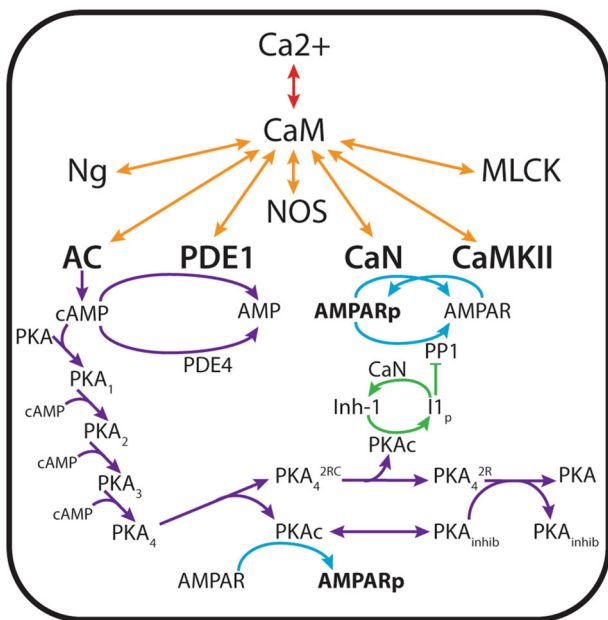
FIGURE 2. Schematic of the CaM-dependent protein signaling network. Ca^{2+} ions flux through the NMDA receptor, initiating a cascade of signaling that results in phosphorylation of the AMPA receptors. CaM-binding proteins (neurogranin (Ng), muscle light chain kinase (MLCK), neuronal nitric oxide synthetase (NOS), calcineurin (CaN, also known as protein phosphatase 3), Ca^{2+}/calmodulin-dependent kinase II (CaMKII), phosphodiesterase 1 (PDE1), adenylyl cyclase 1 (AC1) and adenylyl cyclase 8 (AC8)) simultaneously compete for CaM binding. CaM binding activates the catalytic activity of CaMKII, which phosphorylates the AMPA receptor GluA1 subunit at site S831. Generation of cAMP by CaM-bound adenylyl cyclases activates the catalytic activity of protein kinase A (PKA, also known as cAMP-dependent kinase), which phosphorylates Inh-1 as well as GluA1 at site S845. Phosphodiesterases (both CaM-dependent PDE1 and constitutively active PDE4) regulate intracellular levels of cAMP by hydrolysis, thereby regulating PKA activity. PP1 may additionally de-phosphorylate CaMKII or GluA1. PP1 may become sequestered by Inh-1, until Inh-1 is de-phosphorylated by CaN.

task was to compare a 2-state binding model to that of a 4-state binding model (Figs. 1c and 1d) to validate the hypothesis that the dynamics of CBP binding by CaM are optimally represented by a 4-state binding model. For this, we analyzed model output when stimulated at a frequency of 10 Hz (see Methods). In Fig. 3 we used two metrics to show how the 2-state model (Figs. 3a and 3c) and 4-state model (Figs. 3b and 3d) each responded to 10 Hz Ca^{2+} stimulation. The first metric (Figs. 3a and 3b) monitored CBP binding only to fully-saturated CaM$_4$ over time. The second metric (Figs. 3c and 3d) monitored the total CBP binding to all Ca^{2+}/CaM states. The only difference between metrics for the 2-state model is that the second metric additionally accounts for each CBP bound to apo-CaM (CaM$_0$), if any. Similarly, using the second metric for the 4-state model involves summing

the concentrations of each CBP bound to each Ca^{2+}/CaM state: CaM$_0$, CaM$_{2N}$, CaM$_{2C}$, and CaM$_4$.

By monitoring either CaM$_4$-bound or all CaM-bound CBP, we assessed the added value of a relatively detailed 4-state model to the simpler 2-state model of Ca^{2+}/CaM. In Fig. 3a, each CBP-CaM$_4$ trace exhibited wavelets implying a frequency detection inherent to CBP activation. For most CBPs such as CaN (blue) and AC8ct (black), relative activation by CaM$_4$ generally increased over time, which was consistent with expectation for CBPs exposed to a continuous, frequency-based stimulus. In contrast, Ng (pink) rapidly decreased in relative CaM$_4$ binding over time though this was also expected due to the high affinity of Ng for CaM$_0$ compared to CaM$_4$. In Fig. 3c, the 2-state model elicited similar time-course trends for each CBP compared to Fig. 3a, and because the traces lack frequency-associated wavelets, it appears that CaM$_0$ was significantly bound to CBPs, particularly during inter-spike intervals of Ca^{2+}. The differences between monitoring solely CaM$_4$- vs. all CaM-bound CBPs were further evidenced by Supplemental Fig. S1, which shows equivalent output but for a model stimulated at 50 Hz.

For the 4-state model, the Ca^{2+} frequency-associated waveforms were much more prominent than in the 2-state model (compare Figs. 3b and 3d to Figs. 3a and 3c), indicating that the 4-state model is much more responsive to Ca^{2+} than the 2-state model (some data obscured by the highly dynamic traces). See also results from 50 Hz stimulation in Supplemental Fig. S1. Of note, there is a significant difference in the dynamics of binding of CaM to AC8$_{nt}$ and NOS between the 2-state and 4-state models (compare Figs. 3a and 3c to Figs. 3b and 3c) at 10 Hz. Additionally, the 4-state model is altogether more responsive to rapid changes in Ca^{2+} concentration, even when all the CaM-bound CBPs are summed (Fig. 3d). Taken together this data provides a strong motivation to move forward with the 4-state model as the best model to simulate the frequency-dependent response of CBPs.

Frequency Analysis

Because our current 4-state model dramatically expands on previous work, we wanted to assess the frequency-dependence of CBP activation. We define two metrics in order to compare the frequency response of all CBPs. In the first metric, Normalized C_{b1}, the time-averaged integration of all CaM$_4$-bound CBPs (Equation S1) is normalized to the highest C_{b1} value of each CBP, respectively. In the second metric, Normalized C_{b2}, the time-averaged integration of all CaM species-bound CBPs (Equation S2) is normalized to the

TABLE 1.   Calmodulin binding proteins.

| Protein	Description and chemical reactions
Adenylyl cyclase 1 (AC1)	A prominent adenylyl cyclase isoform in hippocampal neurons. Binds CaM at its C_{1b} domain and, when activated, converts ATP to cAMP[6,7,36,51]
Adenylyl cyclase 8 (AC8)	A prominent adenylyl cyclase isoform in hippocampal neurons. Binds Ca^{2+}/CaM at both its N- and C-termini, which are explicitly accounted for in this work.[16,33] Ca^{2+}/CaM-AC8ct (C-terminus-bound AC8) may bind ATP for conversion to cAMP[36]
Ca^{2+}/CaM-dependent kinase II (CaMKII)	Ca^{2+}/CaM-dependent kinase. Highly expressed in brain, and especially hippocampal tissue.[34] In this work, CaMKII is modeled as monomers which, when active, may dimerize and subsequently become Ca^{2+}/CaM-independent *via* autophosphorylation.[35] Active CaMKII phosphorylates many downstream proteins such as the GluA1 subunit of AMPA receptors[2]
Calcineurin (CaN)	A Ca^{2+}/CaM-dependent serine/threonine phosphatase.[25,50] CaN dephosphorylates GluA1 at S845[3]
Myosin light chain kinase (MLCK)	A putatively abundant CBP in dendritic spines, which we model using kinetic parameters derived from studies on smooth muscle.[10,28,30]
Neurogranin (Ng)	A membrane-associated protein, and one of the few proteins that strongly binds CaM in absence of Ca^{2+}[14,20,44,55]
Nitric oxide synthetase (NOS)	Typically a membrane-associated protein that binds tightly to CaM and generates Nitric Oxide from citrulline and arginine[5,12,40]
Phosphodiesterase 1 (PDE1)	A Ca^{2+}/CaM dependent phosphodiesterase that cleaves cAMP into AMP[8]

TABLE 2.   Non-calmodulin binding proteins included in model.

GluA1	One of four subunits of α-amino-3-hydroxy-5-methyl-4-isoxazolepropionic acid receptor (AMPA receptor). Is phosphorylated at amino acid residue S831 by CaMKII and residue S845 by PKA[18,38] Increase AMPA phosphorylation is implicated in synaptic plasticity, and GluA1-p845 may be necessary for exocytosis of AMPARs to the synaptic membrane[18]
Inhibitor 1 (Inh-1)	When phosphorylated by active PKAc, Inh-1 may bind PP1, inhibiting the ability of PP1 to de-phosphorylate GluA1. Inh-1 is de-phosphorylated by CaM-activated CaN[18]
Phosphodiesterase 4 (PDE4)	PDE4 is not Ca^{2+}/CaM dependent but plays a significant role in regulating the levels of cAMP in cells by cleaving cAMP into AMP. Phosphorylation by active PKAc increases the enzymatic activity of PDE4[17]
PKA inhibitor	A generic model species representative of many unspecified off-target binding partners for PKA. These binding partners sequester PKA, preventing its phosphorylation of GluA1, and they additionally participate in the pathway restoring PKAc to the original four-subunit, auto-regulated PKA heteromer[17]
Protein kinase A (PKA, also known as cAMP-dependent kinase)	Binds up to four cAMP, liberating catalytic subunits that bind and phosphorylate a number of downstream targets such as PDE4, Inh-1, and GluA1[8,38]
Protein phosphatase 1 (PP1)	PP1 de-phosphorylates GluA1 subunits at both S831 and S845, in addition to CaMKII T286.[18] In this model, PP1 may only bind CaMKII when CaMKII is unbound to Ca^{2+}/CaM

highest C_{b2} value of each CBP, respectively. Normalized C_{b1} and C_{b2} values for each CBP are plotted at various Ca^{2+} flux frequencies (Fig. 4).

The frequency responses of the various CBPs, when accounting for all CaM-binding, are in good agreement with previously published results. For example, CaMKII (green trace) exhibited its highest CaM_4-binding (and thus, activation) at high frequencies, peaking around 100 Hz (Figs. 4a and 4b). High frequency activation of CaMKII coincides with the protein's putative role in long-term potentiation, which is initiated under high-frequency (~ 100 Hz) Ca^{2+} flux. Interestingly, Ng, which has a higher affinity for CaM_0 than CaM_4, exhibited relatively little CaM_4-binding across most frequencies, before spiking at about 80 Hz (Figs. 4a and 4c). This spike in average CaM_4-bound Ng is explained by the full saturation of CaM_4 at high frequencies. Indeed, when accounting for all CaM-binding (Fig. 4b), Ng exhibits a peak activation at lower frequencies, which is more consistent with
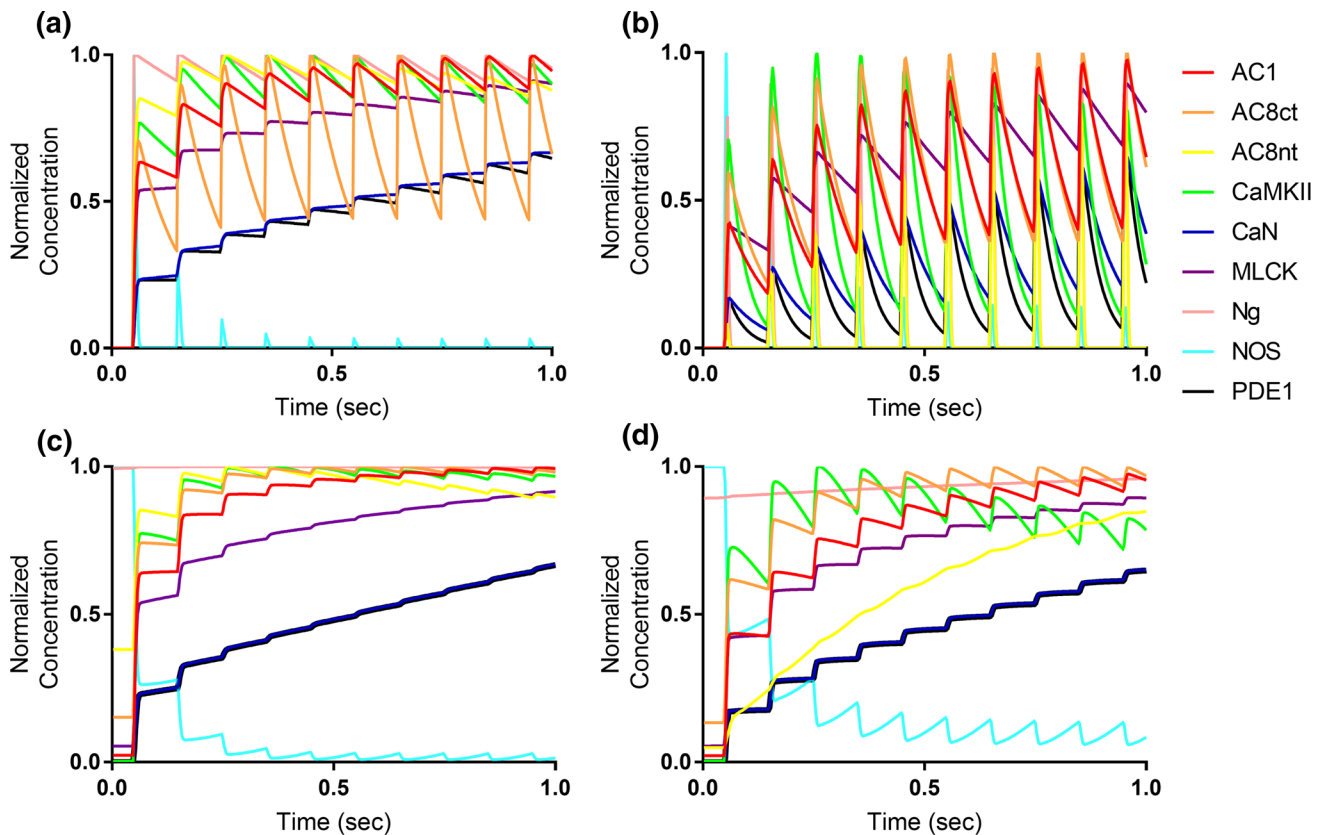
FIGURE 3. Time-course comparison of Ca^{2+}/CaM binding models. (a, b) Response of binding models to 10 Hz Ca^{2+} frequency stimulation, monitoring each CBP bound to Ca^{2+}-saturated CaM$_4$. (c, d) Response of binding models to 10 Hz Ca^{2+} frequency stimulation, monitoring the cumulative concentration of each CBP bound to any Ca^{2+}/CaM state. Similar data for models stimulated at 50 Hz Ca^{2+} is provided in Fig. S1.

expectation.[54] Most notably, when analyzing Normalized C_{b1} (Figs. 4a and 4c) many CBPs such as AC1, AC8, Ng, and NOS have highly similar peak activation frequencies. If distinct Ca^{2+} signals/frequencies elicit activation of distinct Ca^{2+}/CaM-dependent pathways and were in-part dependent on competitive tuning, then we would have expected each CBP to have a more distinguishable frequency of peak activation.

The frequency dependence of the CBPs is clearer when we analyze the data using the second metric, Normalized C_{b2}. As seen in Figs. 4b and 4d, this analysis revealed how CaM$_0$ and the intermediate Ca^{2+}/CaM states can, in conjunction with saturated CaM$_4$, contribute to the frequency-dependence of CBP activation. This is additional evidence that suggests that a 4-state model of Ca^{2+}/CaM binding is able to capture the frequency dependent changes in CBP activation. These results also compare favorably with our previous work.[45] However, in our previous work the adenylyl cyclase CBPs (AC1, AC8$_{nt}$, and AC8$_{ct}$) generally exhibits activation that peaked at higher-frequencies (greater than 50 Hz). In Figs. 4b and 4d, it appears that incorporating the additional CBP (PDE1)

caused a downward shift and sharpening in peak activation frequency for AC8$_{nt}$.

Sensitivity of GluA1 Phosphorylation to Variation in Key Input Parameters

Global sensitivity analysis was performed to assess how variation in input parameters contributed to variation in the overall phosphorylation of GluA1. Latin Hypercube Sampling (LHS) was used to efficiently sample the input parameters over fourfold range (2-fold increased and decreased). Partial Rank Correlation Coefficients (PRCC) was used to quantify how the variation in each input parameter contributed to overall phosphorylation of GluA1 (sum of all phosphorylated GluA1 species). To test the hypothesis that CaMKII significantly contributes to GluA1 phosphorylation under normal Ng concentrations, and PKA (*via* AC1/8 activation of cAMP) significantly contributes to GluA1 phosphorylation when Ng is knocked down, we performed LHS/PRCC analysis under a both wild-type Ng condition and a total Ng KO condition. For both conditions, the parameters
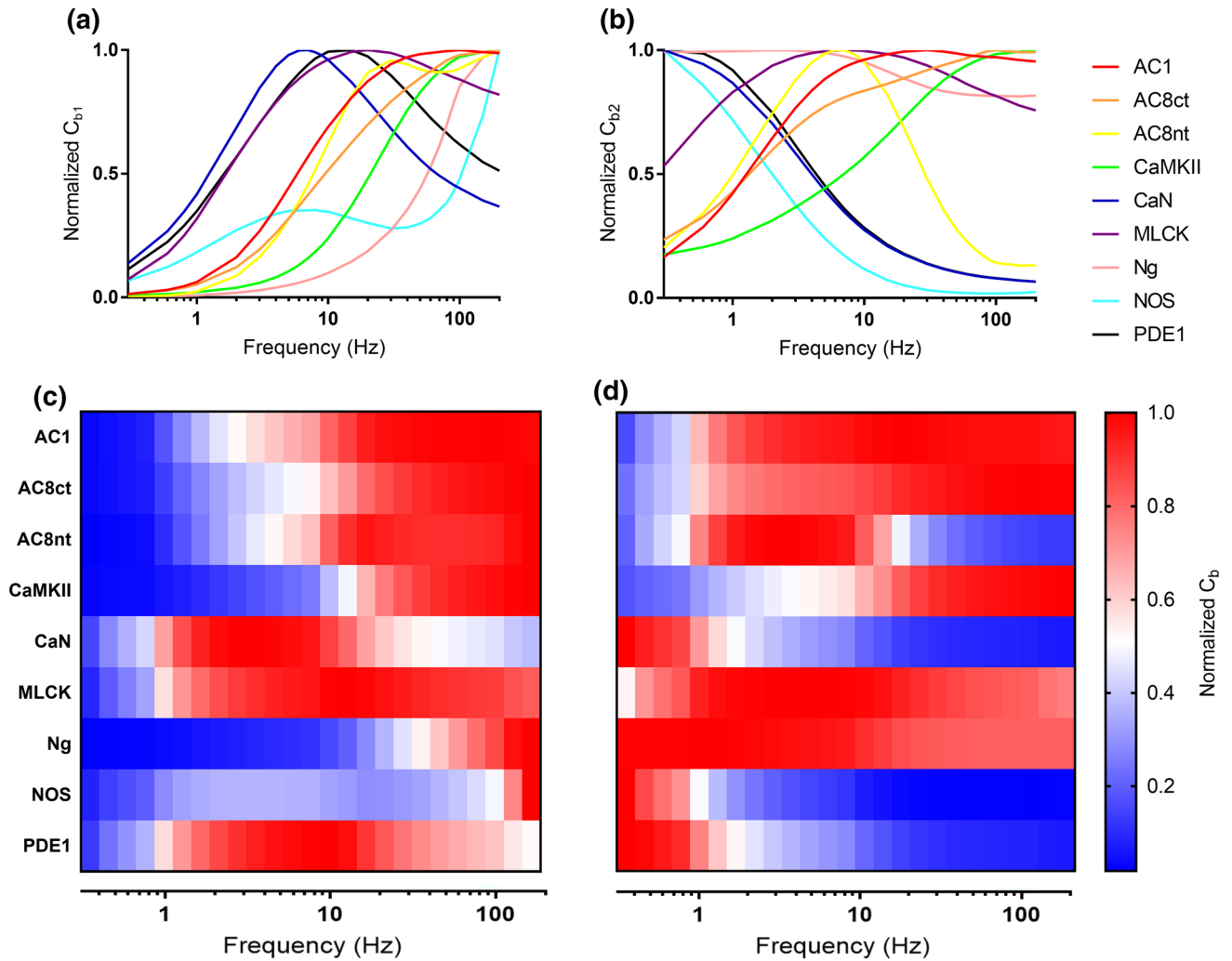
FIGURE 4. Frequency-dependence of CBPs. (a, b) Relative time-averaged concentrations of CaM$_4$-bound CBPs (C$_{b1}$) and all CaM-bound CBPs (C$_{b2}$), respectively, for the 4-state model. (c, d) Heatmap representations of data shown in a and b, where each row denotes the CaM$_4$- and total CaM-binding to each CBP. Blue denotes minimal relative activation of CBP, and red denotes maximal relative activation of CBP. Note the shifts in the frequencies of peak CBP activation when accounting only for CaM$_4$-binding (c) and all CaM-CBP binding (d).

with absolute PRCC's greater than our threshold of 0.5 are shown in Table 3.

In the WT Ng condition at 100 Hz Ca^{2+} flux, all association and catalytic rate parameters (k_{on}^B or k_p^B, where B represents the different CBPs) were varied simultaneously. As expected, we find that the phosphorylation rate constant of CaMKII-mediated phosphorylation of GluA1 $k_p^{KCaM4GluA1}$ is highly correlated with total GluA1 phosphorylation (Table 3). Additionally, the catalytic rate constant for AC1-CaM$_4$ production of cAMP ($k_{on}^{AC1CaM4}$) and that of the downstream output of AC1 activation (PKA, $k_p^{KCaM4GluA1}$) were also highly correlated with phosphorylation of GluA1. This indicates that at 100 Hz and WT Ng conditions, increases in the rate of CaM$_4$

binding to AC1 leads to increases in phosphorylation of GluA1.

For the second set of conditions the concentration of Ng was set to zero to simulate Ng KO. In comparison to the WT Ng case, it is first interesting to note that the phosphorylation rate constant $k_p^{KCaM4GluA1}$ is no longer highly correlated with GluA1 phosphorylation (PRCC value = 0.467, below our threshold of 0.5). Though admittedly this PRCC value for $k_p^{KCaM4GluA1}$ is still somewhat high, its reduction in the Ng KO analysis suggests a diminished importance for CaMKII-mediated phosphorylation of GluA1 subunits. In accordance with our over-arching hypothesis that competitive tuning mediates a shift in pathway activation, we refer again to Table 3 for clues as to the

TABLE 3. Sensitivity analysis of kinetic parameters at 100 Hz Ca^{2+}.

Parameter	Description	PRCC
$k_p^{AC1CaM4}$	Catalytic rate of cAMP production by AC1 bound to CaM_4	0.808
$k_{on}^{AC1CaM4}$	Association rate of AC1 to CaM_4	0.758
$k_p^{PKAcGluA1}$	Catalytic rate of GluA1 phosphorylation by PKAc	0.597
$k_p^{KCaM4GluA1}$	Catalytic rate of GluA1 by CaMKII activated by CaM_4	0.584
$k_{on}^{CaMKIIGluA1}$	Association rate of CaMKII to GluA1	0.527
k_{on}^{KCaM4}	Association rate of CaMKII to CaM_4	-0.732
$k_p^{PDE4cAMP}$	Catalytic rate of cAMP degradation by PDE_4	-0.805

$[Ng] = 0$ Parameter	Description	PRCC
$k_p^{PKAcGluA1}$	Catalytic rate of GluA1 phosphorylation by PKAc	0.785
$k_p^{AC1CaM4}$	Catalytic rate of cAMP production by AC1 bound to CaM_4	0.763
$k_{on}^{PKAcGluA1}$	Association rate of GluA1 to PKAc	0.636
$k_p^{AC8ctCaM4}$	Catalytic rate of cAMP production by AC8-Ct bound to CaM_4	0.618
$k_p^{PDE4cAMP}$	Catalytic rate of cAMP degradation by PDE	-0.864

alternative proteins contributing to GluA1 phosphorylation. Indeed, both the association and catalytic rates of PKAc for GluA1 ($k_{on}^{PKAcGluA1}$ and $k_p^{PKAcGluA1}$, respectively) have significantly greater PRCC values in the Ng KO compared to the WT case. Furthermore, the catalytic rate of cAMP production by $AC8_{ct}$-CaM_4 ($k_p^{ACtctCaM4}$) also exhibits a significant PRCC in the Ng KO case. Note that the short timescale over which we simulate competitive tuning in this sensitivity analysis is biophysically relevant; LTP is classically elicited by a 100 Hz stimulus over one second.[19,21] Additionally, previous models indicate that the predominant Ca^{2+}/CaM state may change in fractions of seconds, which is important considering that each Ca^{2+}/CaM state exhibits significant binding affinities for various CBPs.[42,50] Altogether, the results of our sensitivity analysis indicate that, at least for 100 Hz Ca^{2+} and short timescales (< 2 s), competition for Ca^{2+}/CaM-binding may support a shift in signaling in which Ng perturbation causes AC to overtake CaMKII as the primary activator of pathways leading to GluA1 subunit phosphorylation.

Potential Robustness Provided by Competitive Tuning

Having seen in the preceding sections that our expanded model exhibits similar frequency dependence to a previous result, and that perturbing Ng causes a shift in the parameters most strongly associated with GluA1 phosphorylation, we now explore the functional consequences of competitive tuning in this simplified model of synaptic plasticity. One hallmark of synaptic plasticity is the phosphorylation of AMPAR GluA1 subunits at two residues: S831 and S845. S831 is phosphorylated by CaM-bound CaMKII or pCaMKII, and S845 is phosphorylated by catalytic PKA (PKAc).

Previously we have shown that competitive tuning was able to explain counter-intuitive experimental results showing that Ng genetic knock-out (Ng KO) results in decreased CaMKII activation/autophosphorylation.[45] This same work also predicted that knocking out Ng concentration would cause a shift in CaM binding away from CaMKII in favor of AC8. Noting that activated AC1 and AC8ct generate cAMP, which in turn activates PKA, it seemed that competitive tuning could provide a mechanism for the system to account for perturbations in Ng expression. That is, because Ng KO reduces CaMKII-facilitated phosphorylation of GluA1 S831, competitive tuning could drive the alternative activation of more AC8ct, increasing PKA activation and in turn, phosphorylation of GluA1 S845.

In Fig. 5, we explore this potential mechanism by simulating Ng knockdown, while monitoring the time-averaged concentration of phosphorylated AMPARs (pGluA1) under three different Ca^{2+} flux frequencies. Note that in the simulations for Fig. 5, the number of Ca^{2+} pulses is conserved with varying Ca^{2+} frequency. In order to easily compare across Ca^{2+} frequencies, each panel in Fig. 5 is additionally normalized against the time-averaged pGluA1 concentration observed for the WT Ng case. For all three stimulation frequencies in Fig. 5, GluA1 subunits phosphorylated by CaMKII at S831 (p831, red) decrease with decreasing Ng concentration. As expected, GluA1 phosphorylation by PKAc at S845 (p845, blue) increases with decreasing Ng concentration. However, only for 10 Hz stimulation (Fig. 5a) does the cumulative GluA1 phosphorylation remain relatively constant for all Ng concentrations. Surprisingly, Ng KO caused phos-
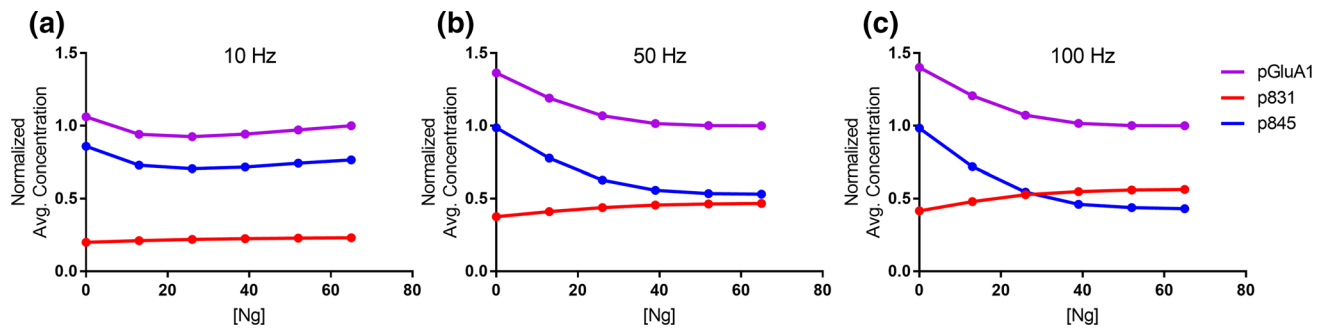
FIGURE 5. Phosphorylation of AMPAR GluA1 Subunits at S831 and S845. Time-averaged concentrations of total phosphorylation (pGluA1, purple), CaMKII-mediated phosphorylation at S831 (p831, red), and PKA-mediated phosphorylation at S845 (p845, blue) against Ng concentration. For each panel, the 4-state Ca^{2+}/CaM binding model was stimulated at either (a) 10 Hz (b) 50 Hz, or (c) 100 Hz Ca^{2+} stimulation. In order to compare Ca^{2+} frequencies, each panel is additionally normalized against the [pGluA1] observed for WT Ng (65 μM).

phorylation at S845 to significantly increase at higher frequencies, whereas the decrease in S831 phosphorylation was relatively modest. It would appear that while competitive tuning could facilitate robustness to perturbations in Ng expression, the system tends to over-correct at early timescales in the absence of additional regulatory mechanisms.

These results imply that high frequency stimulation such as those that elicit LTP (100 Hz) should be more easily attainable upon Ng KO. This result is consistent with Krucker *et al.*,[26] who showed that even though CaMKII activation/phosphorylation is reduced upon Ng KO, long-term potentiation can be achieved following stimulation by only a single 100 Hz tetanus. Further, it is worth noting that for all Ca^{2+} frequencies presenting in Fig. 5, shifts in overall pGluA1 levels with decreasing Ng concentration were largely negligible until Ng expression was reduced by more than half. Thus, it appears that the system is robust to modest perturbations to Ng expression, such as what might be seen in Ng heterozygous animals.

CONCLUSIONS

Competitive tuning is a recently-described phenomenon in which signaling molecules compete for binding of a common activator. Although others have either alluded to or invoked competition as being important in signal transduction,[1,29,49,54] our work shows that competition may play a larger role in informing signaling outcomes than previously thought. In this work we first compare a 2-state and 4-state model of competitive binding for Ca^{2+}/CaM and determined that a 4-state model is best-suited to accurately detect the frequency dependence of a competitive CaM-CBP reaction network under dynamic stimulation. We also verify that expanding our 4-state

model network to include an additional CBPs and downstream species preserves the overall competitive tuning phenomenon. We explore the functional implications of competitive tuning by using sensitivity analysis to identify the parameters most strongly correlated with a hallmark of synaptic plasticity, AMPAR GluA1 subunit phosphorylation. We further explore the implications of competitive tuning by building on a previous result showing that Ng KO counter-intuitively decreases CaMKII activation and autophosphorylation. Because competitive models indicate that Ng KO causes an increase in Ca^{2+}/CaM binding to AC8, we hypothesize that competitive tuning could provide a mechanism that compensates for a loss in CaMKII-mediated phosphorylation of GluA1 by promoting (*via* AC) PKA-mediated phosphorylation of GluA1. Indeed, in Fig. 5 we observe that for high Ca^{2+} flux frequencies, Ng knockdown results in a switch between CaMKII and PKA in cumulative kinase activity.

Interestingly, stimulating at an LTP-inducing Ca^{2+} frequency of 100 Hz (Fig. 5c) further causes an upregulation of GluA1 phosphorylation by PKA in the Ng KO case. This upregulation could explain results by Krucker *et al.* who observed that LTP could be elicited by just a single tetanus of stimulation at 100 Hz in brain slices of Ng KOs. Note that the current model includes both PP1- and CaN-dependent dephosphorylation of GluA1. Contrary to expectation, the combined action of PP1 and Ca^{2+}/CaM-dependent dephosphorylation by CaN seemingly did not dramatically decrease GluA1 phosphorylation levels in the presence of compensation facilitated by competitive tuning. Of course, other regulatory mechanisms could additionally be affecting GluA1 phosphorylation levels. For example, spatial localizations of proteins such as Ng and PP1, or perhaps A-kinase-anchoring proteins (AKAPs), could be required to increase, through

avidity effects, the local concentrations of CaMKII, AC, and/or CaN in the dendritic spine. Alternatively, it may be required to analyze the reaction network presented here on longer timescales in order to discern the complete downstream effects of competitive tuning. As it currently stands, our current results are focused on short-term effects of Ca^{2+}-dependent signaling. Future work is needed to analyze longer term processes (e.g., receptor localization, other feedback mechanisms, receptor trafficking). It remains unclear whether increased GluA1 phosphorylation in Ng KO is an expected consequence of Ng perturbation and represents an example how competitive tuning can impart robustness to model outcomes across a wide range of Ng concentrations, or whether the maintenance of GluA1 phosphorylation is a result of missing layers of model regulation. Future work will include these additional mechanisms of regulation and will explore other protein activation dynamics in GluA1 phosphorylation. A key prediction from our model that could be readily experimentally tested is that the relative level of phosphorylation of GluA1 at p845 would increase in Ng KO mice and phosphorylation of GluA1 at p831 would decrease.

METHODS

Simulation Methods

Chemical reactions between species were written and converted to ordinary differential equations according to laws of mass action using the XCellerator package.[47] Mathematica was used to solve the differential equations using the NDSolve command. All other data analysis (including integration of species concentration over time and the LHS/PRCC sensitivity analysis) were performed in Mathematica (Wolfram Research, Mathematical version 11). Model output is plotted in the 2D graphing program GraphPad Prism (GraphPad, version 7).

Ca^{2+} stimulation was implemented as a boundary condition forcing function for the system of differential equations solved in Mathematica. To control for the magnitude of $^{Ca2+}$ exposure from a single Ca^{2+} pulse, Ca^{2+} spike half widths are set to 5 ms regardless of frequency. To reduce computational complexity and control for the cumulative magnitude of Ca^{2+} exposure across all simulations, total magnitude of calcium flux is conserved at 100 pulses regardless of Ca^{2+} frequency.

All the equations for this model can be found in S1 Appendix. Mathematica files for the complete models can be found on the Purdue PURR database.[43]

Sensitivity Analysis

A global sensitivity analysis was used to investigate how variation in input parameter values contributed to variation in model output. LHS was used to efficiently sample input parameters over a range of values that were determined by experimental measurement or calculated by thermodynamic equilibrium (see Model Parameterization for a more in-depth discussion of model parameterization). In all variations of our sensitivity analysis, each parameter was sampled at least 250 times using values within 2-fold of each parameter's listed value (See S1 Appendix). PRCC were used correlate the rank contribution of parameter variation on the variation in desired model output as described in our previous work.[24,42,45] We have previously shown that allowing the K_d of an interaction to vary by either varying the k_{on} or k_{off} (but not both simultaneously) produced similar results in the sensitivity analysis.[24] Therefore only association rate constants (k_{on}) and catalytic rate constants (k_p) were varied. PRCC analysis produces correlation factors over a range of 1 to -1, where 1 indicates perfect positive correlation and -1 indicates perfect negative correlation. In order to show the parameters whose variation most greatly impacted model output (total phosphorylation of GluA1 AMPAR subunits), a threshold PRCC value of absolute magnitude of 0.5 was used to generate the parameter list in Table 3.

ELECTRONIC SUPPLEMENTARY MATERIAL

The online version of this article (https://doi.org/10.1007/s12195-018-0549-4) contains supplementary material, which is available to authorized users.

CONFLICT OF INTEREST

Authors Matthew Pharris, Neal Patel, and Tamara Kinzer-Ursem declare that they have no conflicts of interest.

ETHICAL STANDARDS

No animal studies were carried out by the authors for this article. Additionally, no human subjects research was conducted in this study.

REFERENCES

[1]Antunes, G., A. C. Roque, and F. M. S. Souza. Modelling intracellular competition for calcium: kinetic and thermodynamic control of different molecular modes of signal decoding. *Sci. Rep.* 6:23730, 2015.

[2]Barria, A., V. Derkach, and T. Soderling. Identification of the Ca^{2+}/calmodulin-dependent protein kinase II regulatory phosphorylation site in the alpha-amino-3-hydroxyl-5-methyl-4-isoxazole-propionate-type glutamate receptor. *J. Biol. Chem.* 272:32727–32730, 1997.

[3]Beattie, E. C., R. C. Carroll, X. Yu, W. Morishita, H. Yasuda, M. von Zastrow, *et al.* Regulation of AMPA receptor endocytosis by a signaling mechanism shared with LTD. *Nat. Neurosci.* 3(12):1291–1300, 2000.

[4]Borlongan, C. V., J. Burns, N. Tajiri, C. E. Stahl, N. L. Weinbren, *et al.* Epidemiological survey-based formulae to approximate incidence and prevalence of neurological disorders in the United States: a meta-analysis. *PLoS ONE* 2:e78490, 2013.

[5]Bredt, D. S., and S. H. Snyder. Isolation of nitric-oxide synthetase, a calmodulin-requiring enzyme. *Proc. Nat. Acad. Sci.* 87(2):682–685, 1990.

[6]Brostrom, C. O., Y. C. Huang, B. M. Breckenridge, and D. J. Wolff. Identification of a calcium-binding protein as a calcium-dependent regulator of brain adenylate cyclase. *Proc. Nat. Acad. Sci.* 72(1):64–68, 1975.

[7]Cali, J. J., J. C. Zwaagstra, N. Mons, D. M. F. Cooper, and J. Krupinski. Type-VIII adenylyl-cyclase - a Ca^{2+}/calmodulin-stimulated enzyme expressed in discrete regions of rat-brain. *J. Biol. Chem.* 269(16):12190–12195, 1994.

[8]Chay, A., I. Zamparo, A. Koschinski, M. Zaccolo, and K. T. Blackwell. Control of beta AR- and *N*-methyl-D-aspartate (NMDA) receptor-dependent cAMP dynamics in hippocampal neurons. *PLoS Comput. Biol.* 12(2):32, 2016.

[9]Chin, D., and A. R. Means. Calmodulin: a prototypical calcium sensor. *Trends Cell Biol.* 10(8):322–328, 2000.

[10]Dabrowska, R., J. M. F. Sherry, D. K. Aromatorio, and D. J. Hartshorne. Modulator protein as a component of myosin light chain kinase from chicken gizzard. *Biochemistry* 17(2):253–258, 1978.

[11]Diering, G. H., S. Heo, N. K. Hussain, B. Liu, and R. L. Huganir. Extensive phosphorylation of AMPA receptors in neurons. *Proc. Nat. Acad. Sci.* 113(33):4920–4927, 2016.

[12]Doyle, C. A., and P. Slater. Localization of neuronal and endothelial nitric oxide synthase isoforms in human hippocampus. *Neuroscience* 76(2):387–395, 1997.

[13]Forest, A., M. T. Swulius, J. K. Y. Tse, J. M. Bradshaw, T. Gaertner, and M. N. Waxham. Role of the N- and C-lobes of calmodulin in the activation of Ca^{2+}/calmodulin-dependent protein kinase II. *Biochemistry* 47(40):10587–10599, 2008.

[14]Gerendasy, D. D., S. R. Herron, J. B. Watson, and J. G. Sutcliffe. Mutational and biophysical studies suggest RC3/neurogranin regulates calmodulin availability. *J. Biol. Chem.* 269(35):22420–22426, 1994.

[15]Ghosh, A., and M. E. Greenberg. Calcium signaling in neurons: molecular mechanisms and cellular consequences. *Science* 268(5208):239–247, 1995.

[16]Gu, C., and D. M. F. Cooper. Calmodulin-binding sites on adenylyl cyclase type VIII. *J. Biol. Chem.* 274(12):8012–8021, 1999.

[17]Hao, H. P., D. E. Zak, T. Sauter, J. Schwaber, and B. A. Ogunnaike. Modeling the VPAC(2)-activated cAMP/PKA signaling pathway: from receptor to circadian clock gene induction. *Biophys. J.* 90(5):1560–1571, 2006.

[18]Hayer, A., and U. S. Bhalla. Molecular switches at the synapse emerge from receptor and kinase traffic. *PLoS Comput. Biol.* 1(2):137–154, 2005.

[19]Herring, B. E., and R. A. Nicoll. Long-term potentiation: from CaMKII to AMPA receptor trafficking. *Ann. Rev. Physiol.* 78:351–365, 2016.

[20]Huang, K. P., F. L. Huang, and H. C. Chen. Characterization of a 7.5-kDa protein-kinase-C substrate (RC3 protein, neurogranin) from rat-brain. *Arch. Biochem. Biophys.* 305(2):570–580, 1993.

[21]Huganir, R. L., and R. A. Nicoll. Ampars and synaptic plasticity: the last 25 years. *Neuron* 80(3):704–717, 2013.

[22]Keller, D. X., K. M. Franks, T. M. Bartol, and T. J. Sejnowski. Calmodulin activation by calcium transients in the postsynaptic density of dendritic spines. *PLoS ONE* 3(4):16, 2008.

[23]Kim, M., A. J. Park, R. Havekes, A. Chay, L. A. Guercio, R. F. Oliveira, *et al.* Colocalization of protein kinase A with adenylyl cyclase enhances protein kinase A activity during induction of long-lasting long-term potentiation. *PLoS Comput. Biol.* 7(6):18, 2011.

[24]Kinzer-Ursem, T. L., and J. J. Linderman. Both ligand- and cell-specific parameters control ligand agonism in a kinetic model of G protein-coupled receptor signaling. *PLoS Comput. Biol.* 3(1):84–94, 2007.

[25]Klee, C. B., and M. H. Krinks. Purification of cyclic 3′,5′-nucleotide phosphodiesterase inhibitory protein by affinity chromatography on activator protein coupled to sepharose. *Biochemistry* 17(1):120–126, 1978.

[26]Krucker, T., G. R. Siggins, R. K. McNamara, K. A. Lindsley, A. Dao, D. W. Allison, *et al.* Targeted disruption of RC3 reveals a calmodulin-based mechanism for regulating metaplasticity in the hippocampus. *J. Neurosci.* 22(13):5525–5535, 2002.

[27]Kulkami, C., M. Lo, J. G. Fraseur, D. A. Tirrell, and T. L. Kinzer-Ursem. Bioorthogonal chemoenzymatic functionalization of calmodulin for bioconjugation applications. *Bioconj Chem.* 26(10):2153–2160, 2015.

[28]Lei, S. B., E. Czerwinska, W. Czerwinski, M. P. Walsh, and J. F. MacDonald. Regulation of NMDA receptor activity by F-actin and myosin light chain kinase. *J. Neurosci.* 21(21):8464–8472, 2001.

[29]Li, L., M. I. Stefan, and N. Le Novere. Calcium input frequency, duration and amplitude differentially modulate the relative activation of calcineurin and CaMKII. *PLoS ONE* 7(9):17, 2012.

[30]Lukas, T. J., W. H. Burgess, F. G. Prendergast, W. Lau, and D. M. Watterson. Calmodulin binding domains: characterization of a phosphorylation and calmodulin binding-site from myosin light chain kinase. *Biochemistry* 25(6):1458–1464, 1986.

[31]Malenka, R. C., B. Lancaster, and R. S. Zucker. Temporal limits on the rise in postsynaptic calcium required for the induction of long-term potentiation. *Neuron* 9(1):121–128, 1992.

[32]Maravall, M., Z. F. Mainen, B. L. Sabatini, and K. Svoboda. Estimating intracellular calcium concentrations and buffering without wavelength ratioing. *Biophys. J.* 78(5):2655–2667, 2000.

[33]Masada, N., S. Schaks, S. E. Jackson, A. Sinz, and D. M. F. Cooper. Distinct mechanisms of calmodulin binding and regulation of adenylyl cyclases 1 and 8. *Biochemistry* 51(40):7917–7929, 2012.

[34]Miller, S. G., and M. B. Kennedy. Distinct forebrain and cerebellar isozymes of type II Ca²⁺/calmodulin-dependent protein kinase associate differently with the postsynaptic density fraction. *J. Biol. Chem.* 260(15):9039–9046, 1985.

[35]Miller, S. G., and M. B. Kennedy. Regulation of brain type-II Ca²⁺/calmodulin-dependent protein-kinase by autophosphorylation: a Ca²⁺-triggered molecular switch. *Cell* 44(6):861–870, 1986.

[36]Mons, N., M. Yoshimura, and D. M. F. Cooper. Discrete expression of Ca²⁺/calmodulin-sensitive and Ca²⁺-insensitive adenylyl cyclases in the rat-brain. *Synapse* 14(1):51–59, 1993.

[37]Nabavi, S., H. W. Kessels, S. Alfonso, J. Aow, R. Fox, and R. Malinow. Metabotropic NMDA receptor function is required for NMDA receptor-dependent long-term depression. *Proc. Nat. Acad. Sci.* 110(10):4027–4032, 2013.

[38]Oliveira, R. F., M. Kim, and K. T. Blackwell. Subcellular location of PKA controls striatal plasticity: stochastic simulations in spiny dendrites. *PLoS Comput. Biol.* 8(2):19, 2012.

[39]Olwin, B. B., A. M. Edelman, E. G. Krebs, and D. R. Storm. Quantitation of energy coupling between Ca²⁺, calmodulin, skeletal-muscle myosin light chain kinase, and kinase substrates. *J. Biol. Chem.* 259(17):949–955, 1984.

[40]Panda, K., S. Ghosh, and D. J. Stuehr. Calmodulin activates intersubunit electron transfer in the neuronal nitric-oxide synthase dimer. *J. Biol. Chem.* 276(26):23349–23356, 2001.

[41]Peersen, O. B., T. S. Madsen, and J. J. Falke. Intermolecular tuning of calmodulin by target peptides and proteins: differential effects on Ca²⁺ binding and implications for kinase activation. *Protein Sci.* 6(4):794–807, 1997.

[42]Pepke, S., T. Kinzer-Ursem, S. Mihalas, and M. B. Kennedy. A dynamic model of interactions of Ca²⁺, calmod-

ulin, and catalytic subunits of Ca²⁺/Calmodulin-dependent protein kinase II. *PLoS Comput. Biol.* 6(2):15, 2010.

[43]Pharris, M. C., N. M. Patel, and T. L. Kinzer-Ursem. Competitive tuning of Ca²⁺/calmodulin-activated proteins provides a compensatory mechanism for AMPA receptor phosphorylation in synaptic plasticity. Purdue University Research Repository. https://doi.org/10.4231/r7st7n11.

[44]Represa, A., J. C. Deloulme, M. Sensenbrenner, Y. Benari, and J. Baudier. Neurogranin: immunocytochemical localization of a brain-specific protein-kinase-c substrate. *J. Neurosci.* 10(12):3782–3792, 1990.

[45]Romano, D. R., M. C. Pharris, N. M. Patel, and T. L. Kinzer-Ursem. Competitive tuning: competition's role in setting the frequency-dependence of Ca²⁺-dependent proteins. *PLoS Comput. Biol.* 13(11):10–45, 2017.

[46]Saucerman, J. J., and D. M. Bers. Calmodulin mediates differential sensitivity of CaMKII and calcineurin to local Ca²⁺ in cardiac myocytes. *Biophys. J.* 95(10):4597–4612, 2008.

[47]Shapiro, B. E., A. Levchenko, E. M. Meyerowitz, B. J. Wold, and E. D. Mjolsness. Cellerator: extending a computer algebra system to include biochemical arrows for signal transduction simulations. *Bioinformatics* 19(5):677–678, 2003.

[48]Shifman, J. M., M. H. Choi, S. Mihalas, S. L. Mayo, and M. B. Kennedy. Ca²⁺/calmodulin-dependent protein kinase II (CaMKII) is activated by calmodulin with two bound calciums. *Proc. Nat. Acad. Sci.* 103(38):13968–13973, 2006.

[49]Slavov, N., J. Carey, and S. Linse. Calmodulin transduces Ca²⁺ oscillations into differential regulation of its target proteins. *ACS Chem. Neurosci.* 4(4):601–612, 2013.

[50]Stemmer, P. M., and C. B. Klee. Dual calcium ion regulation of calcineurin by calmodulin and calcineurin B. *Biochemistry* 33(22):6859–6866, 1994.

[51]Swislocki, N. I., and J. Tierney. Solubilization, stabilization, and partial-purification of brain adenylate cyclase from rat. *Biochemistry* 12(10):1862–1866, 1973.

[52]WHO. Neurological Disorders: Public Health Challenges. Geneva: WHO Press, 2006.

[53]Xia, Z. G., and D. R. Storm. The role of calmodulin as a signal integrator for synaptic plasticity. *Nat. Rev. Neurosci.* 6(4):267–276, 1995.

[54]Zhabotinsky, A. M., R. N. Camp, I. R. Epstein, and J. E. Lisman. Role of the neurogranin concentrated in spines in the induction of long-term potentiation. *J. Neurosci.* 26(28):7337–7347, 2006.

[55]Zhong, L., and N. Z. Gerges. Neurogranin targets calmodulin and lowers the threshold for the induction of long-term potentiation. *PLoS ONE* 7(7):8, 2012.